

An earth fault location method based on negative sequence voltage changes at low voltage side of distribution transformers

David Topolánek^a, Matti Lehtonen^b, Petr Toman^a, Jaroslava Orsagova^a, Jiri Drapela^a

^a Brno University of Technology, Faculty of Electrical Engineering and Communication, Brno, Czech Republic

^b Aalto University, Aalto, Finland

ARTICLE INFO

Keywords:

Earth fault
Fault localization
Voltage monitor
Distribution network
Negative sequence voltage
Distribution transformer
Voltage dip

ABSTRACT

The paper presents a new approach for earth fault localization which is based on evaluation of phase to ground voltages recorded by voltage monitors installed at low-voltage side of distribution transformer station deployed under smart metering projects. The introduced method “Vdip” determines the probability of asymmetrical fault location based on comparison of the changes in negative sequence current recorded at the feeding medium voltage substation and changes in negative sequence voltages recorded at the LV sides of distribution transformers. The paper describes the nature of the method and presents its principle using simulation of a MV resonant earthed distribution network where short-term connection of an auxiliary resistor is used. The method was also evaluated in real resonant earthed 22 kV network, where totally 15 earth faults with fault resistance up to 1.2 kΩ were carried out. As the result of this field test, the location error of the Vdip method is presented.

1. Introduction

Despite decades of experience with operation of resonant earthed medium voltage (MV) distribution networks, fast and accurate location of an earth fault (EF) in such networks is still very challenging. This is due to a high complexity of distribution networks caused by its purpose of distribution of electrical energy to all customers and relatively low earth fault currents due to reactive component compensation. At the present time, the identification of faulty feeder at supply substation is relatively reliable; however localization of the earth fault on affected feeder is not suitably solved.

One of the most widespread and most effective methods for EF localization is still trial switching, i.e. successive process of disconnection and reclosing of individual feeder sections until the fault is found. This multiple switching operation has negative impact to the continuity of power supply and can cause subsequent EF or short circuit due to switching over-voltages and elevated voltages on the two healthy phases.

Another technical solution for an EF localization utilizes fault indicator units. Those devices can indicate the EF direction based on monitoring of voltage and current specific parameters [12]. The size of indicated faulty area depends on the number of installed indicators and their arrangement within the DS, which requires a large number of installed monitors to achieve satisfactory results. Another disadvantage

is the necessity of other supplementary means like trial switching for the final localization of the fault by an operator in the selected part of the network in the case of a small number of fault indicators and complicated fault location in the case of malfunction of one of installed indicators.

The next group of the means intended for EF location in a DS is based on calculation of a fault loop impedance/reactance on faulty feeder [3–6]. Resulting reactance calculated by a locator (IED - Intelligent Electronic Device) is used for estimation of distance to the fault. However the calculated electrical distance can correspond to more than one possible faulty point. Therefore complementary method has to be applied, as it was introduced in [7] or base on smart meters measurement in [8]. Similar problem is characteristic also for travelling wave based methods [9–12], where precise time synchronization has to be employed.

On the other hand, the voltage monitors, newly installed into distribution transformer stations (DTS), in recent years, bring new possibilities in the fault location task. The primary purpose of those devices is to monitor the voltage and power conditions including voltage and power quality indices at the low voltage (LV) site of DTS. Some monitors also support basic functions to indicate non-standard operation states in the LV network (e.g. MV fuse failure, over/under voltage etc.) or to remotely control LV circuit breakers or a tap changer of on-load tap changer transformer. However, in order to maximize the

E-mail addresses: topolane@feec.vutbr.cz (D. Topolánek), matti.lehtonen@aalto.fi (M. Lehtonen), toman@feec.vutbr.cz (P. Toman), orsagova@feec.vutbr.cz (J. Orsagova), drapela@feec.vutbr.cz (J. Drapela).

<https://doi.org/10.1016/j.ijepes.2019.105768>

Received 14 June 2019; Received in revised form 22 October 2019; Accepted 9 December 2019

0142-0615/ © 2019 Elsevier Ltd. All rights reserved.

benefits of those devices (DTS monitors), it is necessary to gradually implement useful functions that would allow distribution system operator (DSO) to improve both the voltage quality and the power supply continuity. The method presented in this paper (Vdip method) is designed to utilize at data set measured by the voltage monitors for EF localization purpose, which may significantly increase the benefits of DTS monitors and thus satisfy investments in the monitoring systems. Some other methods focused on evaluation of recorded voltage dips for fault localization were introduced in contributions [13,14], where voltage dip database is used for estimation of a fault location. This solution requires the creation of an extensive voltage dip database on the basis of which the pattern of recorded voltage dips is searched to find likely fault location. However, the proposed approach of the Vdip method does not require the creation of a voltage dip database. The fault location is determined by means of comparison of voltage dips calculated for given fault condition utilizing current recorded on the faulty feeder with voltage dips recorded in available DTSs.

Another way to localize fault based on recorded voltage and current condition is described in [15], where iterative load flow algorithm is used for estimation of fault state voltage distribution for all evaluated faulty points/nodes in DS. This estimated voltage database is then utilized for selection of likely fault location by consideration of mismatches of measured and estimated nodal voltages. Similar method, where fault resistance is necessary additionally to estimate, is presented also in [16] and [17]. Both of those concepts are different from presented method, because the Vdip method utilizes node voltage method which is applied to negative sequence scheme, whereas current recorded on the feeder is directly used for calculation of negative sequence voltage distribution. This is a reason, why load estimation and subsequent iterative steady state calculation is not necessary to use.

Method based on pre-fault and fault analyses of voltages monitored by smart meters installed along the feeder is presented in [18] and [19]. This method is similar to described method Vdip, but it is designed only for localization of short circuits in MV solidly earthed DSs, where comprehensive sensing method is applied for fault point position estimation. Location of earth faults in resonant earthed DS is not studied. Another difference from the Vdip method, there is a possibility to localize the fault only on buses, while localization of the fault along lengthy feeder is not solved. In contrast, the Vdip method can be used for localization of an earth fault located anywhere in compensated networks, because auxiliary nodes and appropriate change in phasor of negative sequence voltage is utilized as Section 2 and Section 3 present.

Another method [20] is based on optimization process which estimates post-fault steady state (including load admittances, equivalent current sources etc.) to minimize error between recorded and estimated voltage phasors quantities on a feeder. In the case of Vdip method, it is not necessary to estimate post-fault steady state reflecting load current distribution in the network. Proposed method utilizes only difference between two immediately consecutive states (pre-fault and fault states or fault states without and with connected auxiliary resistor), therefore impact of load flow to the Vdip method accuracy is eliminated. Moreover, method [20] is neither suitable nor intended for localization of earth faults in compensated DSs.

The main difference of proposed method in comparison with those above mentioned can be generally summarized as follows:

- The Vdip method is suitable and dedicated for an earth fault localization in extensive mixed (cable/over head line) resonant earthed MV networks, which are characterized by low level of an earth fault current (commonly in tens of amps) and low density of measuring points (points where voltage condition can be monitored).
- An earth fault can be localized on the long feeder or its laterals, because the Vdip method uses segmentation of a network topology (see Fig. 3).
- Location of an earth fault is determined based on change in negative sequence voltage and current, that minimize negative impact of

stochastic loads in DS (the change is estimated as a difference between two moving averaging windows shifted in the range from 0.06 to 0.3 s).

- Proposed method is not suitable for localization of three-phase short circuit type of faults, it can be used only for localization of asymmetrical faults (in terms of resonant earthed DS it means an earth fault, double earth fault or line to line short circuit type fault).

2. The nature of the Vdip method for an earth fault location

As described in the introduction, development of measurement in DTS offers new possibilities for distribution system analysis in both LV and MV networks. Nowadays question of earth fault location in MV networks is not satisfactorily solved due to complexity of MV networks and insufficient number of installed fault indicators. The problem of EF localization is a very interesting area in which improvements could be made by utilizing data from voltage monitors installed in DTSs. In case that the measurement on the secondary side of MV/LV distribution transformer (DT) is going to be used, the localization method may be based on analysis of the voltage unbalance measured as negative sequence component at the system fundamental frequency. As it was introduced, positive or zero sequence component can be used as well for earth fault localization purpose in MV DS. Unfortunately, zero sequence voltage component is not transferred from MV to LV side of DT in common Dyn connection and also zero sequence analysis based methods are affected by the significant error due to the MV network zero sequence impedance estimation uncertainty. Therefore methods or analysis utilizing zero sequence component are insufficient for EF location technique employing voltage monitoring on the LV side of DT. As well as the positive sequence voltage magnitude can be more influenced by three-phase high power load switching or on-load tap positions changes in comparison to corresponding negative sequence voltage. Impacts of those events have to be suppressed, because they can significantly affect the localization process. Furthermore, negative sequence voltage component has lower dynamic range of magnitude, which is constrained by voltage unbalance limit (according to EN 50160 the limit for negative sequence component magnitude at system fundamental frequency is 2% of the positive sequence component), therefore utilization of negative sequence component rather than the positive one was chosen as more appropriate.

From the fault localization point of view, the voltage negative sequence magnitude can be influenced only by asymmetrical faults, where in terms of widely used resonant earthed distribution network it is an earth fault, double earth fault or line to line short circuit. The monitoring of the negative sequence voltage at LV side of DTs can be used for localization of all these asymmetrical faults. Therefore the method introduced in [21] was improved.

The case of an earth fault described by means of symmetrical components is shown in Fig. 2, which is created for the simple distribution network showed in Fig. 1. The figure shows a resonant earthed MV distribution network with additional resistor R_A for short-time increasing of active part of earth fault current. The network comprises of

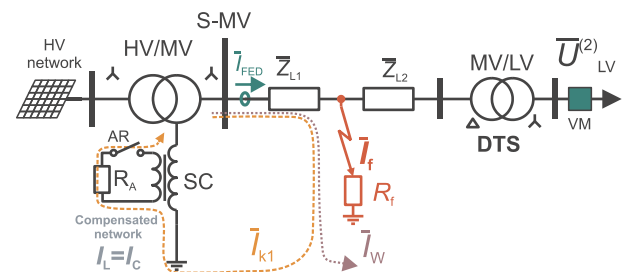


Fig. 1. Resonant earthed MV distribution network with automatics for short-time connection of auxiliary resistor.

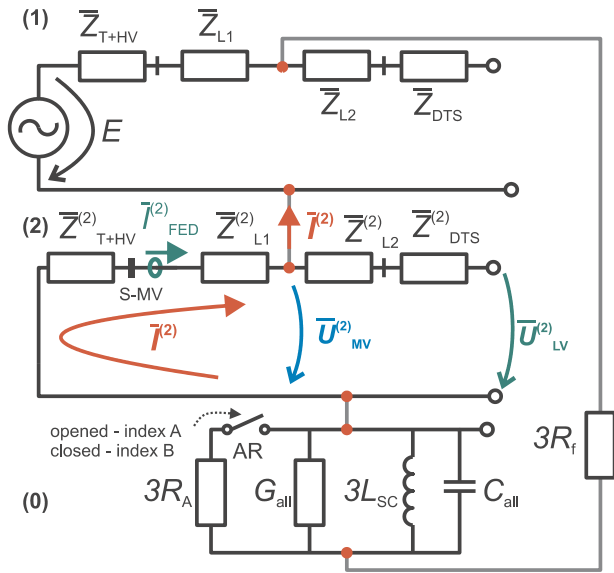


Fig. 2. Symmetrical component scheme of the network affected by an earth fault.

only one feeder, where phase currents I_{FED} are measured in supply substation, and one DTS is placed at the end of the feeder, where voltage monitor (VM) is installed at LV side providing negative voltage $U^{(2)}$ monitoring, as Fig. 1 shows.

Assuming that the feeder is affected by an earth fault, the residual current I_w flows through the feeder as presented in Fig. 1. This case is also described by the symmetrical component scheme showed in Fig. 2, where impact of LV load and capacitances of positive and negative sequence impedance network is neglected to keep maximal simplicity. As presented in this scheme (Fig. 2), the negative sequence of fault current $I^{(2)}$ causes voltage drop $\bar{U}_{MV}^{(2)}$ on relevant negative sequence impedance, which is transferred on LV side of DTS as voltage $\bar{U}_{LV}^{(2)}$, where $\bar{U}_{LV}^{(2)} = \bar{U}_{LV}^{(2)} \cdot r_{MV/LV}$ and $r_{MV/LV}$ is the actual ratio of DT.

In a case that the auxiliary resistor R_A is connected by the circuit-breaker (AR in Fig. 2) for 1 s (it is used to increase ability of earth fault detection by feeder protection), the magnitude of negative sequence current $I^{(2)}$ and also voltage $\bar{U}_{LV}^{(2)}$ is increased.

Respecting presumption that negative sequence of the line capacitance is neglected as it can be seen in Fig. 2, the negative sequence current measured at the beginning of faulty feeder $I_{FED}^{(2)}$ is equal to the negative sequence of fault current $I^{(2)}$. Therefore only variable $I_{FED}^{(2)}$ is used for further explanation.

The influence of load fluctuation on monitored values $I_{FED}^{(2)}$ and $\bar{U}_{LV}^{(2)}$ can be eliminated by evaluation of the change in negative sequence current $\Delta I_{FED}^{(2)}$ and voltage $\Delta U_{LV}^{(2)}$ before and after auxiliary resistor connection (AR in Fig. 2) according to (1)

$$\begin{aligned} \Delta U_{LV}^{(2)} &= |\bar{U}_{LV(B)}^{(2)} - \bar{U}_{LV(A)}^{(2)}| \\ \Delta I_{FED}^{(2)} &= |\bar{I}_{FED(B)}^{(2)} - \bar{I}_{FED(A)}^{(2)}| \end{aligned} \quad (1)$$

where index A means state without auxiliary resistor R_A and B with R_A . If both the changes are known, i.e. $\Delta I_{FED}^{(2)}$ monitored in supply substation and $\Delta U_{LV}^{(2)}$ on the secondary side of DTS, the estimation of the fault location is achievable based on negative sequence impedance scheme. The fault can be localized at the point of the line, where current $\Delta I_{FED}^{(2)}$ causes same change in negative sequence voltage $\Delta U_{LV}^{(2)}$ as it is measured on the LV side of DTS. The similar principle (1) can be applied to a pre-fault (A) and fault state (B) of any asymmetrical fault.

The designed principle for earth fault localization is described in more details in chapter 3 using the node-voltage analysis. With respect to the voltage dip that occurs on the secondary side of the DTS during asymmetrical faults, the method is called ‘‘Vdip’’.

3. The Vdip method principle

The Vdip method is designed to determine the probability of EF location based on the evaluation of the recorded changes of negative sequence current $\Delta I_{FED}^{(2)}$ and voltage $\Delta U_{LV}^{(2)}$ according to (1). As indicated in chapter 2, the values $\Delta U_{LV}^{(2)}$ are monitored and recorded at the secondary side of selected MV/LV DTs by means of VMs and $\Delta I_{FED}^{(2)}$ value is monitored and recorded at the faulty feeder in the supplying MV substation. The $\Delta I_{FED}^{(2)}$ value can be determined from post processing of fault records provided by the feeder protection signaling or tripping the fault. To ensure correct localization, there is necessary to record at least one $\Delta U_{LV}^{(2)}$ in DTS behind the fault (related to supply nodes as presented in Fig. 1).

3.1. Numerical model formulation for Vdip method

The numerical model for the Vdip method is based on negative sequence scheme of the monitored system. In the first step, let's neglect the shunt admittances of the line as presented in Fig. 1 respectively in Fig. 2, in this case $\bar{I}_{FED}^{(2)} = \bar{I}^{(2)}$. Then, in order to remove the positive and zero-sequence from symmetrical component scheme depicted in Fig. 2, it is possible to substitute both of this sequence scheme parts by a simple current source with magnitude of the negative sequence current $\bar{I}_{FED}^{(2)}$ respectively $\Delta I_{FED}^{(2)}$ (1) flowing through the faulty feeder and monitored at the supply substation (S-MV in Fig. 2). This simplified scheme can be seen in Fig. 3, where $\Delta I_{FED}^{(2)}$ evokes voltage change $\Delta U_{LV}^{(2)}$, whereas $\bar{Z}_{T+HV}^{(2)}$ is negative short-circuit impedance of the high voltage (HV) network including impedance of supply HV/MV transformer, $\bar{Z}_{L1}^{(2)}$ is negative impedance of the monitored feeder and $\bar{Z}_{DTS}^{(2)}$ is negative impedance of MV/LV DT. Just this optimized negative sequence scheme is suitable for Vdip method application.

In the first step, each line section (line impedance) of the network is divided into individual elements with maximal length Δ (e.g. 0.1 km) as it is presented in Fig. 3. It creates auxiliary nodes (UP) where the probability of fault presence is calculated by the method. It is worth to note, that the accuracy of the Vdip algorithm is higher for the shorter length of Δ elements (fault point can be identified with higher resolution). The corresponding negative sequence admittance matrix $[\bar{Y}^{(2)}]$ can be created for this optimized negative sequence scheme of tested network. Then the node-voltage analysis is applied consequently, calculating negative voltages at the LV side of DT for any presumed fault location (for all UP and UM nodes), i.e. current source is step by step connected to all nodes UP and UM, while $\Delta \bar{U}_{LV}^{(2)}$ is calculated (see Fig. 3). Comparing calculated differences $|\Delta \bar{U}_{LV}^{(2)}|$ with measured ones allows to determine the probability of an asymmetrical fault location as it is described in Section 3.2.

3.2. Asymmetrical fault location probability calculation

The principle of the Vdip method is based on stepwise connection of the fault point (node EF in Fig. 3) to the individual virtual nodes numbered 1 to n , where n is total number of UP including UM nodes (UM is measuring node i.e. node where VM is installed). Therefore the following Eq. (2) formulated according to node-voltage method is

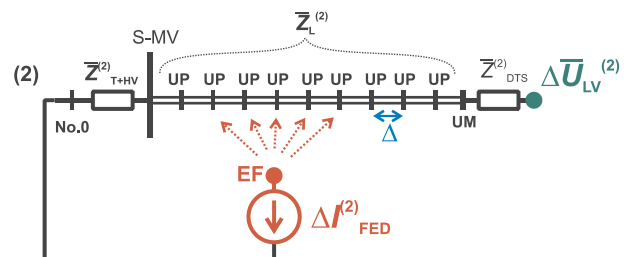


Fig. 3. Negative sequence scheme optimized for Vdip method.

solved for node $N = 1, 2, \dots, n$, where N is index of the node number with considered EF location, i.e. node where negative current source is connected.

$$\begin{bmatrix} [\Delta\bar{U}_{UM}^{(2)}] \\ [\Delta\bar{U}_{UP}^{(2)}] \end{bmatrix}^{(N)} = [\bar{Y}^{(2)}]^{-1} \cdot [\Delta I_{FED}^{(2)}]^{(N)} \quad (2)$$

where $[\Delta\bar{U}_{UM}^{(2)}]^{(N)}$ is a vector of calculated changes in negative sequence voltage in measuring nodes UM when fault is considered in node N ($N = 1, 2, \dots, n$), $[\Delta\bar{U}_{UP}^{(2)}]^{(N)}$ is a vector of calculated changes in negative sequence voltage in inspected UP nodes when fault is considered in node N ($N = 1, 2, \dots, n$) and $[\Delta I_{FED}^{(2)}]^{(N)}$ is vector of change in negative sequence current assembled for fault in the node N ($N = 1, 2, \dots, n$).

Supposing an earth fault in node 1 ($N = 1$), the Eq. (2) can be transcribed to (3) and (4), where $\Delta I_{FED}^{(2)}$ is determined according to (1) from fault record of $\bar{I}_{FED}^{(2)}$:

$$[\Delta\bar{U}_{UM}^{(2)}]^{(1)} = \begin{bmatrix} \Delta\bar{U}_{UM1}^{(2)} \\ \Delta\bar{U}_{UM2}^{(2)} \\ \vdots \\ \Delta\bar{U}_{UMi}^{(2)} \end{bmatrix}^{(1)}, \quad [\Delta\bar{U}_{UP}^{(2)}]^{(1)} = \begin{bmatrix} \Delta\bar{U}_{UP(i+1)}^{(2)} \\ \Delta\bar{U}_{UP(i+2)}^{(2)} \\ \vdots \\ \Delta\bar{U}_{UPn}^{(2)} \end{bmatrix}^{(1)} \quad (3)$$

$$[\Delta I_{FED}^{(2)}]^{(1)} = \begin{bmatrix} 1_i [\Delta I_{FED}^{(2)}]^{(1)} \\ \vdots \\ 1_{(i+1)} [\Delta I_{FED}^{(2)}]^{(1)} \\ \vdots \\ 1_n [\Delta I_{FED}^{(2)}]^{(1)} \end{bmatrix} = \begin{bmatrix} -\Delta I_{FED}^{(2)} \\ 0 \\ \vdots \\ 0 \\ 0 \\ \vdots \\ 0 \end{bmatrix}^{(1)} \quad (4)$$

Inverse negative sequence admittance matrix can be decomposed to four sub-matrices according to number of UM nodes as it is shown in (5):

$$[\bar{Y}^{(2)}]^{-1} = \begin{bmatrix} [\bar{Y}_{inv1}^{(2)}] & [\bar{Y}_{inv2}^{(2)}] \\ [\bar{Y}_{inv3}^{(2)}] & [\bar{Y}_{inv4}^{(2)}] \end{bmatrix} = \begin{bmatrix} \begin{bmatrix} \bar{Y}_{11}^{(2)} & \dots & \bar{Y}_{1i}^{(2)} \\ \vdots & \ddots & \vdots \\ \bar{Y}_{i1}^{(2)} & \dots & \bar{Y}_{ii}^{(2)} \end{bmatrix} & \begin{bmatrix} \bar{Y}_{1(i+1)}^{(2)} & \dots & \bar{Y}_{1n}^{(2)} \\ \vdots & \ddots & \vdots \\ \bar{Y}_{i(i+1)}^{(2)} & \dots & \bar{Y}_{in}^{(2)} \end{bmatrix} \\ \begin{bmatrix} \bar{Y}_{(i+1)1}^{(2)} & \dots & \bar{Y}_{(i+1)i}^{(2)} \\ \vdots & \ddots & \vdots \\ \bar{Y}_{n1}^{(2)} & \dots & \bar{Y}_{ni}^{(2)} \end{bmatrix} & \begin{bmatrix} \bar{Y}_{(i+1)(i+1)}^{(2)} & \dots & \bar{Y}_{(i+1)n}^{(2)} \\ \vdots & \ddots & \vdots \\ \bar{Y}_{n(i+1)}^{(2)} & \dots & \bar{Y}_{nn}^{(2)} \end{bmatrix} \end{bmatrix} \quad (5)$$

where i is number of used voltage monitors (UM nodes).

For faster and more effective calculation of the matrix $[\Delta\bar{U}_{UM}^{(2)}]^{(N)}$, which is needed to quantify the probability of the fault location, formula (2) can be modified to form (6).

$$[\Delta\bar{U}_{UM}^{(2)}]^{(N)} = [\bar{Y}_{inv1}^{(2)}]^{-1} \cdot 1_i [\Delta I_{FED}^{(2)}]^{(N)} + [\bar{Y}_{inv2}^{(2)}]^{-1} \cdot 1_{(i+1)} [\Delta I_{FED}^{(2)}]^{(N)} \quad (6)$$

In the first step of the method, the Eq. (6) is calculated for all respected fault positions i.e. nodes $N = 1, 2, \dots, n$.

The next step solves the Eq. (7) for $N = 1, 2, \dots, n$. This equation calculates the deviation (error), which is given by the difference between the calculated and measured values of change in negative sequence voltage for each UM node considering earth fault in node 1 through n .

$$[\varepsilon]^{(N)} = [|\Delta\bar{U}_{UM}^{(2)}|]^{(N)} - [\Delta U_{MV}^{(2)}] \quad (7)$$

where $[\varepsilon]^{(N)}$ is vector of deviations for all nodes UM in case of fault in node N ($N = 1, 2, \dots, n$), $[\Delta U_{MV}^{(2)}]$ is vector of measured change in negative sequence voltage in respected UM nodes recalculated to MV side of distribution transformer, see (1) where $\Delta U_{MV}^{(2)} = \Delta U_{LV}^{(2)} \cdot r_{MV/LV}$.

Eq. (8) shows individual elements of matrixes presented in (7).

$$\begin{bmatrix} \varepsilon_1^{(N)} \\ \varepsilon_2^{(N)} \\ \vdots \\ \varepsilon_i^{(N)} \end{bmatrix} = \begin{bmatrix} |\Delta\bar{U}_{UM1}^{(2)}|^{(N)} \\ |\Delta\bar{U}_{UM2}^{(2)}|^{(N)} \\ \vdots \\ |\Delta\bar{U}_{UMi}^{(2)}|^{(N)} \end{bmatrix} - \begin{bmatrix} \Delta U_{MV1}^{(2)} \\ \Delta U_{MV2}^{(2)} \\ \vdots \\ \Delta U_{MVi}^{(2)} \end{bmatrix} \quad (8)$$

In the next step, vector of total error $[E]$ is calculated based on deviations $[\varepsilon]^{(N)}$. The vector $[E]$ expresses total error/difference between measured and calculated values of the change in negative sequence voltage of monitored network for individual nodes $N = 1, 2, \dots, n$ as shown in (9).

$$[E] = \begin{bmatrix} E_1 \\ E_2 \\ \vdots \\ E_N \end{bmatrix} = \begin{bmatrix} \sum_{p=1}^i |\varepsilon_p^{(1)}| \\ \sum_{p=1}^i |\varepsilon_p^{(2)}| \\ \vdots \\ \sum_{p=1}^i |\varepsilon_p^{(N)}| \end{bmatrix} N \quad (9)$$

Finally, percentage value of probability of fault presence F is calculated for each node N according to (10)

$$F_N = \frac{E_{\max} - E_N}{E_{\max} - E_{\min}} \cdot 100 \quad (10)$$

where E_{\max} and E_{\min} are maximal and minimal values of the vector $[E]$ respectively, E_N is value of total error for individual node N .

Node with the highest probability (100%) is then selected as the faulty point. Analogically, based on the F values and their distribution, the probability of fault location can be expressed for all nodes (UP and UM). That could be used for presentation of the results in dispatcher GIS systems or in other user interfaces as graphical presentation of location probability distribution on the network scheme. Principle of the Vdp method is protected by European patent [22].

3.3. Infeed negative sequence current correction

The principle of the method was described in Section 3.1 and Section 3.2 with respect of negligible shunt admittance of the feeder ($\bar{Y}_{FED}^{(2)} = 0$ S). This presumption is not correct for feeders composed of cables or long overhead lines, where shunt capacitance eventually conductance reaches significant value. Just in this case, shunt admittance has to be incorporated into negative sequence admittance matrix and the negative sequence current magnitude, which is used as infeed for optimized negative sequence scheme in Fig. 3, has to be corrected according to (11)

$$\begin{aligned} \Delta I_{FED_C}^{(2)} &= \Delta I_{FED}^{(2)} \cdot |1 + \bar{Z}_{T+HV}^{(2)} \cdot \bar{Y}_{FED}^{(2)}| \\ \bar{Y}_{FED}^{(2)} &= \sum \bar{Y}_L^{(2)} \end{aligned} \quad (11)$$

where $\bar{Y}_L^{(2)}$ is line shunt admittance of individual section of the monitored feeder.

The Eq. (11) was derived from the negative sequence scheme presented in Fig. 4, where impact of the line impedance is neglected. As shown, the monitored $\Delta I_{FED}^{(2)}$ (1) has to be increased by the part of the negative sequence current which is flowing through the shunt admittance of the faulty feeder. This corrected current magnitude $\Delta I_{FED_C}^{(2)}$

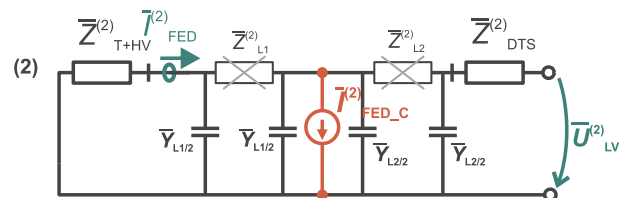


Fig. 4. Negative sequence current magnitude correction.

is then used for current source of optimized negative sequence scheme in Fig. 3.

The impact of the line impedance on negative sequence current distribution is reduced by evaluation of the current change in two states which are shifted by the minimum time (e.g. 0.3 s) as expressed in (1).

4. Verification of the Vdip method

The above introduced Vdip method was verified using both numerical simulation and field tests in a resonant earthed 22 kV DS which were carried out in 2018 [23]. The main aim of the simulation was to verify the theoretical assumptions and to demonstrate the method principle under simplified operating conditions i.e. in steady states, without influence of load and distributed energy resources (DER). The aim of field tests was to verify performance of the method under real dynamic conditions due to variable loads, DER etc. and under realistic asymmetrical operational conditions. The results of both tests are discussed in the Sections 4.1 and 4.2.

4.1. Verification of modelled resonant earthed MV network

The Vdip method is verified by means of simulation of a 22 kV resonant earthed DS, which is modeled in PSCAD Professional to ensure evaluation of the method sensitivity (ability to detect high resistance earth faults) before its deployment in real distribution system; simplified scheme is shown in Fig. 5. This simple DS model consists of six 22/0.4 kV DTSs equipped with models of VMs on their LV side evaluating change in negative sequence voltage. Topology of the test network and position of each DTS were chosen with respect to the Czech MV compensated networks common topology. Supply 110/22 kV substation consists of three outgoing feeders V1, V2 and one feeder presenting the rest of mixed network (60 km of overhead and 90 km of cable lines). The feeder V1 is operated in basic state as radial, where five fault points (F1 to F5) are modeled for simulation of earth faults (short-circuit faults weren't assumed). Last fault point F6 is situated on the MV supply substation busbar.

The second feeder V2 is designed for reconfiguration of the network from radial to ring connection by closing of disconnecter CB. This reconfiguration allows to evaluate the impact on Vdip method sensitivity. Both the feeders V1 and V2 are overhead lines with homogenous impedance (0.245 + j0.36) Ω/km. The arc-suppression coil is ideally tuned to capacitive current of 215 A. In this state, the EF current is compensated to 20 A (residual current respects ca. 10% of network capacitive current). The auxiliary resistor with resistance of 350 Ω is modeled in parallel with arc-suppression coil. This value provides increase of fault (residual) current to 57 A (37 A resistor current). The resistor is connected in 1.5 s after EF ignition for 1 s interval, described timing is in consonance with common setting of auxiliary resistor automatics used in the Czech DS. Negative sequence short circuit impedance of the feeder to MV supply substation $Z_{T+HV}^{(2)} = j1.38 \Omega$ is used.

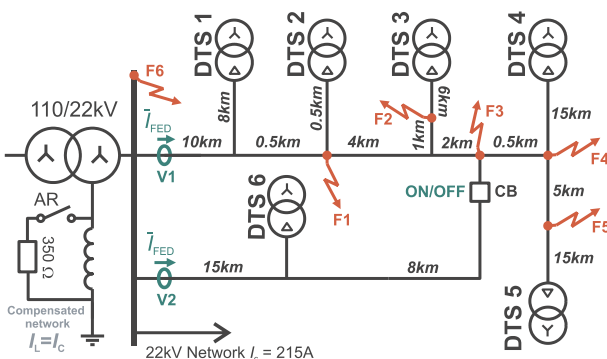


Fig. 5. Simplified scheme of resonant earthed MV network.

Table 1 Vdip input parameters and location error for radial network configuration.

Fault point no.	R_f [Ω]	$\Delta U_{MV}^{(2)}$ [V]					$\Delta I_{FED}^{(2)}$ [A]	Error [km]	
		DTS 1	DTS 2	DTS 3	DTS 4	DTS 5			
1	10	62.6	65.1	64.9	64.8	64.8	15.6	11.3	-0.1
2	10	61.8	64.3	88.3	83.3	83.3	15.4	11.2	-0.1
3	10	61.7	64.1	83.2	92.8	92.7	15.4	11.1	-0.1
4	10	61.6	64.0	83.1	95.1	95.0	15.3	11.1	-0.1
5	10	61.0	63.4	82.3	94.1	118.0	15.2	11.0	-0.1
6	10	16.0	16.0	15.9	15.9	15.9	16.1	0.0	X
1	200	28.0	29.1	29.0	29.0	28.9	7.0	5.0	-0.1
2	200	27.7	28.8	39.6	37.4	37.3	6.9	5.0	-0.1
3	200	27.7	28.8	37.4	41.6	41.6	6.9	5.0	-0.1
4	200	27.7	28.8	37.3	42.7	42.7	6.9	5.0	-0.1
5	200	27.5	28.6	37.1	42.4	53.2	6.9	5.0	-0.1
6	200	6.9	6.9	6.9	6.9	6.9	7.0	0.0	X
1	400	15.7	16.4	16.3	16.3	16.3	4.0	2.8	0.0
2	400	15.7	16.3	22.3	21.1	21.1	3.9	2.8	0.0
3	400	15.6	16.2	21.1	23.5	23.5	3.9	2.8	-0.1
4	400	15.6	16.2	21.1	24.1	24.1	3.9	2.8	-0.1
5	400	15.6	16.2	21.0	24.0	30.0	3.9	2.8	-0.1
6	400	3.8	3.8	3.8	3.8	3.8	3.8	0.0	X
1	600	10.2	10.6	10.6	10.5	10.5	2.6	1.8	0.0
2	600	10.1	10.5	14.4	13.6	13.6	2.6	1.8	0.0
3	600	10.1	10.5	13.6	15.2	15.2	2.6	1.8	0.0
4	600	10.1	10.5	13.6	15.6	15.6	2.6	1.8	0.0
5	600	10.1	10.5	13.6	15.5	19.4	2.6	1.8	0.0
6	600	2.4	2.4	2.4	2.4	2.4	2.4	0.0	X
1	1000	5.3	5.5	5.5	5.5	5.5	1.4	1.0	0.1
2	1000	5.3	5.5	7.6	7.1	7.1	1.4	0.9	0.1
3	1000	5.3	5.5	7.1	7.9	7.9	1.4	0.9	0.0
4	1000	5.3	5.5	7.1	8.1	8.1	1.4	0.9	0.0
5	1000	5.3	5.5	7.1	8.1	10.2	1.4	0.9	0.0
6	1000	1.2	1.2	1.2	1.2	1.2	1.2	0.0	X

In order to obtain the input data for the Vdip method verification, the earth faults with resistance of 10 Ω, 200 Ω, 400 Ω, 600 Ω and 1 kΩ were subsequently simulated in all respected points F1 to F6. For the whole set of faults, voltage and current negative sequence changes caused by auxiliary resistor connection were assessed from simulation results according to (1), where $\Delta I_{FED}^{(2)}$ results from the vector sum of negative sequence currents of both feeders V1 and V2. RMS values of these changes are documented for all tests in Table 1 (radial configuration of the network - CB opened) and Table 2 (ring configuration - CB closed). An example of the RMS values of negative sequence voltage/current trends obtained from simulation of 10 Ω earth fault at F5 point of the radial network is shown in Fig. 6 (EF ignition in $t = 0.5$ s, auxiliary resistor connection in $t = 2$ s).

Then the EF location is estimated based on the input data (Tab. 1 and Tab. 2) employing procedure described in Section 3 with segmentation of lines $\Delta = 0.1$ km. The localization error, which is presented in Table 1 and 2, was expressed as deviation between estimated and correct place of the fault to present the performance of the Vdip method under the given scenarios. Negative value of localization error means estimation of the fault closer to supply substation.

As the results listed in Tables 1 and 2 demonstrate, the correct fault points were identified in all tests with localization error ranging from -200 to 200 m, taking into account used segmentation of 100 m.

4.2. Pilot test in the real resonant earthed MV network

From the real application of the method point of view, it is necessary to solve the issue of influence of variable unbalanced load to Vdip method (correct determination of $\Delta U_{LV}^{(2)}$), which was not considered for shake of simplicity in the simulations. Practical verification of the Vdip method in real 22 kV compensated DS was the subject of field test performed in 2018 whose results (localization errors) are presented in

Table 2
Vdip input parameters and location error for ring network configuration.

Fault point no.	R_f [Ω]	$\Delta U_{MV}^{(2)}$ [V]						$\Delta I_{FED}^{(2)}$ [A]	Error [km]
		DTS 1	DTS 2	DTS 3	DTS 4	DTS 5	DTS 6		
1	10	49.8	51.7	46.4	43.8	43.8	33.6	11.4	-0.1
2	10	44.6	46.2	63.3	54.8	54.8	40.6	11.3	-0.1
3	10	42.2	43.7	54.9	60.5	60.5	44.3	11.3	-0.2
4	10	42.2	43.6	54.8	62.9	62.8	44.3	11.3	-0.1
5	10	41.8	43.2	54.3	62.3	86.4	43.8	11.2	-0.1
6	10	15.9	15.9	15.9	15.9	15.9	15.9	0.0	X
1	200	22.4	23.2	20.9	19.7	19.7	15.1	5.1	0.0
2	200	20.1	20.8	28.5	24.7	24.6	18.3	5.1	0.0
3	200	19.0	19.7	24.7	27.2	27.2	20.0	5.1	-0.1
4	200	19.0	19.7	24.7	28.3	28.3	19.9	5.0	0.0
5	200	18.9	19.6	24.5	28.1	38.9	19.8	5.0	0.0
6	200	6.9	6.9	6.9	6.9	6.9	6.9	0.0	X
1	400	12.6	13.1	11.8	11.1	11.1	8.5	2.8	0.0
2	400	11.3	11.7	16.0	13.9	13.9	10.3	2.8	0.0
3	400	10.7	11.1	13.9	15.3	15.3	11.3	2.8	0.0
4	400	10.7	11.1	13.9	15.9	15.9	11.2	2.8	0.0
5	400	10.7	11.0	13.8	15.8	21.9	11.2	2.8	0.0
6	400	3.8	3.8	3.8	3.8	3.8	3.8	0.0	X
1	600	8.2	8.5	7.6	7.2	7.2	5.5	1.8	0.1
2	600	7.3	7.6	10.4	9.0	9.0	6.7	1.8	0.0
3	600	6.9	7.2	9.0	9.9	9.9	7.3	1.8	0.0
4	600	6.9	7.2	9.0	10.3	10.3	7.3	1.8	0.0
5	600	6.9	7.1	9.0	10.3	14.2	7.3	1.8	0.0
6	600	2.4	2.4	2.4	2.4	2.4	2.4	0.0	X
1	1000	4.3	4.4	4.0	3.8	3.8	2.9	1.0	0.2
2	1000	3.8	4.0	5.4	4.7	4.7	3.5	1.0	0.1
3	1000	3.6	3.8	4.7	5.2	5.2	3.8	1.0	0.1
4	1000	3.6	3.8	4.7	5.4	5.4	3.8	1.0	0.1
5	1000	3.6	3.7	4.7	5.4	7.4	3.8	1.0	0.1
6	1000	1.2	1.2	1.2	1.2	1.2	1.2	0.0	X

Table 3. Thanks to the ring topology of the network, two configurations of the radial feeder were possible to test. In the case of the first radial feeder configuration, the earth fault was 35 km distant from supply substation and 23 km in the case of the second one. The arc suppression coil was equipped by an auxiliary resistor similarly to the simulation. The value of auxiliary resistor R_p on secondary winding of the arc-suppression coil was alternatively 0.5 Ω or 1 Ω (i.e. seen as 353 Ω and 707 Ω on primary side, respectively) (Table 3). The capacitive current of the network was 80 A and the system was ideally tuned (without

Table 3
Location error and test configuration in the real resonant earthed network.

Test	EF character	Additional resistor/Configuration	Location error [km]
1	1.2 k Ω	$R_p = 0.5 \Omega/35$ km to EF	-0.40
2	430 Ω	$R_p = 0.5 \Omega/35$ km to EF	-1.19
3	210 Ω	$R_p = 0.5 \Omega/35$ km to EF	-1.19
4	arcing	$R_p = 0.5 \Omega/35$ km to EF	-0.80
5	direct EF, 13 Ω	$R_p = 0.5 \Omega/35$ km to EF	-0.60
6	1.1 k Ω	$R_p = 1 \Omega/35$ km to EF	-1.19
7	440 Ω	$R_p = 1 \Omega/35$ km to EF	-2.19
8	280 Ω	$R_p = 1 \Omega/35$ km to EF	-0.60
9	arcing	$R_p = 1 \Omega/35$ km to EF	-1.39
10	direct EF, 13 Ω	$R_p = 1 \Omega/35$ km to EF	-0.80
11	1.1 k Ω	$R_p = 1 \Omega/23$ km to EF	-2.80
12	430 Ω	$R_p = 1 \Omega/23$ km to EF	0.20
13	270 Ω	$R_p = 1 \Omega/23$ km to EF	-0.64
14	arcing	$R_p = 1 \Omega/23$ km to EF	-0.19
15	direct EF, 13 Ω	$R_p = 1 \Omega/23$ km to EF	-1.75
Average location error [km]			1.06

detuning). In total 15 tests in three configurations were carried out within one day, where each configuration was of different type of an EF: resistive EF (fault resistance from 1.5 k Ω to 200 Ω), arcing/intermittent EF or direct contact to earthing system with resistance of 13 Ω (see Table 3 - EF character). It can be seen, that there are no significant differences in the localization error caused by different value of auxiliary resistor (0.5 Ω vs. 1 Ω) or distance to EF (35 km vs. 23 km). Resulting absolute location error varies from 200 m to 2.8 km, with a mean value of 1.06 km, respecting segmentation of $\Delta = 0.2$ km. These localization errors are definitely acceptable from dispatcher's point of view and therefore the Vdip method significantly contributes to improving of power supply continuity. A more detailed description of those results, data acquisition and information about the pilot test are presented in [23].

4.3. Evaluation of the method performance

Similar methods based on voltage dip evaluation were introduced in [13–20], unfortunately those fault localization methods were designed or tested only under short-circuit conditions. Therefore, relevant benchmark tests aimed at earth faults localization in compensated networks, that could be used to compare the proposed method with methods [13–20], are not available. Since the aim of the proposed Vdip

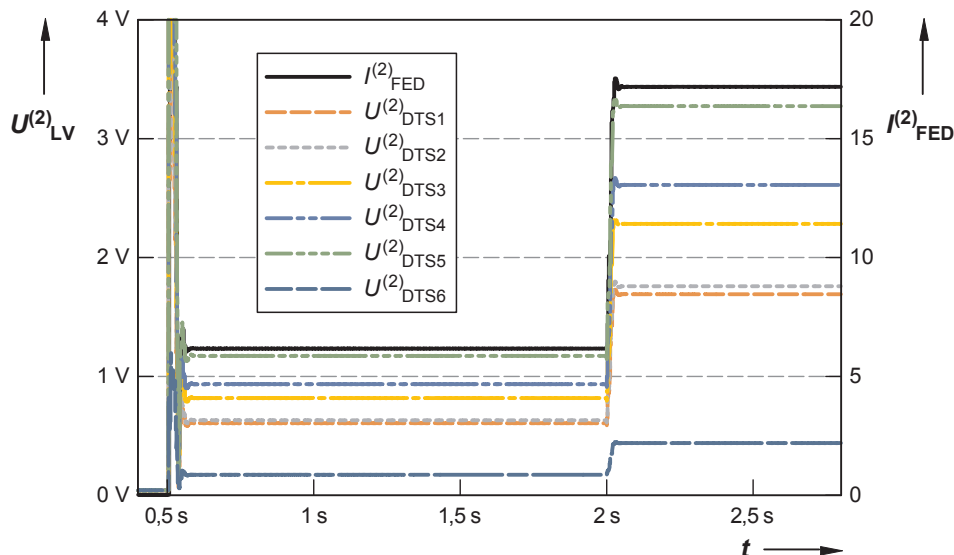


Fig. 6. Curve of negative sequence voltage and current magnitudes before and during 10 Ω earth fault in F5 of radial network.

method is primarily to solve the issue of localization of earth faults, the tests of Vdip method were focused mainly on the verification of the ability to locate high resistance earth faults in resonant earthed MV networks not only in the simulation but also in real operating conditions. The experience gained will be primarily used for optimization of the algorithm intended for detection and recording of the change in negative sequence voltage used in voltage monitors, which is crucial in order to achieve sensitive and accurate fault localization. Theoretical assumptions of the method and the experience obtained from both the simulation and the pilot test can be used for formulation of following advantages and disadvantages of the method.

Pros:

- Possibility of high-impedance earth fault localization, simulations and pilot test showed that successful localization of EF with resistance up to 1 k Ω is feasible (negative load impact on the method sensitivity can be reduced by the number of installed VMs).
- It is not necessary to use data from all installed measuring points (VMs) for earth fault localization purpose, because only VMs placed behind the fault play a key role.
- Reliable EF localization is possible even on long feeders and laterals with the use of optional segmentation Δ .
- Computation time for fault location from received measured data in common MV DS size is within 1 s (the calculation time for EF localization in the pilot test was up to 20 ms, where total line length was 57 km and segmentation 0.2 km, i.e. 285 nodes).
- Except localization of EF, the Vdip method can be used also for asymmetric (short-circuit) faults localization (not tested, but we can assume several times higher sensitivity and accuracy of the method with respect to common fault current levels).
- Detuning of arc-suppression coil did not significantly affect the accuracy of the Vdip method (lower sensitivity was observed in case of under-compensated state).

Cons:

- Location error can be significantly influenced by stochastic behavior of DS (loads fluctuation, switching operations, on-load tap positions changes, etc.). Due to the DS operation stochasticity, the localization error can range in the order of km (illustrated by experimental measurements in Table 3). This could be a challenge in topologically complicated networks. Ideally, the fault location can be assumed in the order of 0.1 km.
- The sensitivity of the method decreases with the EF proximity to supply substation (the resulting voltage dip can be hidden in measurement noise). This issue can be addressed by robustness of implemented algorithms for analysis of the U and I negative sequence components in used voltage monitors.
- In a ring of meshed networks, the sensitivity of EF location is significantly reduced, because the negative sequence current is decreased due to its spreading into branches.
- Other disadvantages are more likely relevant to a monitoring system which provides recorded data to the Vdip method:
 - o necessity to perform precise post-processing synchronization of U and I fault records (especially in case of intermittent or arcing EF);
 - o data affected by the load stochasticity has to be filtered/deleted (records affected by the change in load current unbalance cannot be used as an input for Vdip method), high number of such affected records may reduce the localization accuracy of the method.

5. Conclusion

In view of the unsatisfactory problem of L-N faults localization in distribution systems at the present, the introduced method can significantly contribute to improving the continuity of power supply and

corresponding SAIFI/SAIDI system indices.

The satisfactory benefit of the method should be localization of earth faults with an error which allows to delimitate faulty section without necessity of trial switching and hence of multiple supply interruptions. As it is demonstrated by the results of the pilot test, this goal has been achieved in condition of the real 22 kV resonant earthed network, where average earth fault location error was 1.06 km respecting fault resistance up to 1.2 k Ω . These results demonstrate high potential of the method to reducing of the time required to earth fault localization in MV distribution network.

Since there is not any currently applied or available method, respectively earth fault localization system, that could localize high-resistance earth faults in resonant earthed systems with similar accuracy, it is possible to expect significant contribution of the method especially in the area of localization of earth faults with fault resistance up to 1.5 k Ω in resonant earth distribution network equipped by an auxiliary resistor. Significantly better performance of the Vdip method, in case of L-N fault localization, can be further expected in low-resistor earthed or solidly earthed systems due to higher fault current magnitudes which are prospective in such networks.

With regard to benefits, the Vdip method can be applied to any distribution system (compensated, isolated, resistor or solidly earthed), where it is possible to use already existing voltage monitors without the need of their replacement in all DTSS. Correct performance of the method can be ensured by voltage monitors which are placed at the end of the feeders or lateral lines, while the fault record (of $\Delta U_{12}^{(2)}$) obtained from at least one voltage monitor placed behind the fault is only necessary to use for acceptable fault localization precision. It means that failure of any single monitor may not affect the result of the Vdip method.

Declaration of Competing Interest

The authors declare the following financial interests/personal relationships which may be considered as potential competing interests: The paper describes a new method for localization of asymmetric faults (Vdip method), which is protected by European Patent No. EP2940483. There is financial interest of author's employer Brno University of Technology flowing from selling of the patent license. For the first time this paper describes in detail the nature of the Vdip method on the basis of which the claims for a European patent were formulated. Therefore this contribution is complemented to the EP.

Acknowledgment

This research work has been carried out in the Centre for Research and Utilization of Renewable Energy (CVVOZE). Authors gratefully acknowledge financial support from the Ministry of Education, Youth and Sports of the Czech Republic under BUT specific research programme (project No. FEKT-S-17-4784).

References

- [1] Farughian A, Kumpulainen L, Kauhaniemi K. Review of methodologies for earth fault indication and location in compensated and unearthed MV distribution networks. *Electric Power Syst Res* 2018;154:373–80. ISSN 0378-7796.
- [2] Teng J, Huang W, Luan S. Automatic and fast faulted line-section location method for distribution systems based on fault indicators. *IEEE Trans Power Syst* July 2014;29(4):1653–62.
- [3] Aboshady FM, Thomas DWP, Sumner M. A new single end wideband impedance based fault location scheme for distribution systems. *Electric Power Syst Res* 2019;173:263–70. ISSN 0378-7796.
- [4] de Aguiar Rodrigo Alves, Dalcastagné André Luís, Zürn Hans Helmut, Seara Rui. Impedance-based fault location methods: Sensitivity analysis and performance improvement. *Electr Power Syst Res* 2018;155:236–45. <https://doi.org/10.1016/j.epsr.2017.10.021>.
- [5] Terzija V, Radojević ZM, Preston G. Flexible synchronized measurement technology-based fault locator. *IEEE Trans Smart Grid* March 2015;6(2):866–73.
- [6] Jia K, Thomas D, Sumner M. A new single-ended fault-location scheme for

- utilization in an integrated power system. *IEEE Trans Power Delivery* Jan. 2013;28(1):38–46.
- [7] Morales-Espana G, Mora-Florez J, Vargas-Torres H. Elimination of multiple estimation for fault location in radial power systems by using fundamental single-end measurements. *IEEE Trans Power Delivery* July 2009;24(3):1382–9.
- [8] Trindade FCL, Freitas W. Low voltage zones to support fault location in distribution systems with smart meters. *IEEE Trans Smart Grid* Nov. 2017;8(6):2765–74.
- [9] Shi S, Zhu B, Lei A, Dong X. Fault location for radial distribution network via topology and reclosure-generating traveling waves. *IEEE Trans Smart Grid* 2019.
- [10] Liang Rui, Wang Zheng, Peng Nan, Zare Firuz, Liu Xiaowen, Liu Chenglei. Traveling wave protection based on asynchronously sampled time difference of arrival of modulus traveling waves in per unit line length. *Electr Power Syst Res* 2018;165:250–8. <https://doi.org/10.1016/j.epsr.2018.08.013>.
- [11] Peng Nan, Zhou Lutian, Liang Rui, Xu Haoyuan. Fault location of transmission lines connecting with short branches based on polarity and arrival time of asynchronously recorded traveling waves. *Electr Power Syst Res* 2019;169:184–94. <https://doi.org/10.1016/j.epsr.2018.12.022>.
- [12] Galijasevic Z, Abur A. Fault area estimation via intelligent processing of fault-induced transients. *IEEE Trans Power Syst* Nov. 2003;18(4):1241–7.
- [13] Awal LJ, Mokhlis H, Halim AHA. Improved fault location on distribution network based on multiple measurements of voltage sags pattern. *Power and Energy (PECon)*. IEEE International Conference. 2012. p. 767–72.
- [14] Li H, Mokhar AS, Jenkins N. Automatic fault location on distribution network using voltage sags measurements. *Electricity Distribution*, 2005. CIRED 2005. 18th International Conference and Exhibition. 2005. p. 6–9.
- [15] Pereira RAF, da Silva LGW, Kezunovic M, Mantovani JRS. Improved Fault Location on Distribution Feeders Based on Matching During-Fault Voltage Sags. *IEEE Trans Power Delivery* April 2009;24(2):852–62.
- [16] Lotfifard S, Kezunovic M, Mousavi MJ. Voltage sag data utilization for distribution fault location. *IEEE Trans. Power Del.* Apr. 2011;26(2):1239–46.
- [17] Chen P, Malbasa V, Dong Y, Kezunovic M. Sensitivity analysis of voltage sag based fault location with distributed generation. *IEEE Trans Smart Grid* July 2015;6(4):2098–106.
- [18] Majidi M, Arabali A, Etezadi-Amoli M. Fault location in distribution networks by compressive sensing. *IEEE Trans Power Del* Aug. 2015;30(4):1761–9.
- [19] Majidi M, Etezadi-Amoli M, Sami Fadali M. A novel method for single and simultaneous fault location in distribution networks. *IEEE Trans Power Syst* 2015;30(6):3368–76.
- [20] Manassero G, Di Santo SG, Souto L. Heuristic method for fault location in distribution feeders with the presence of distributed generation. *IEEE Trans Smart Grid* Nov. 2017;8(6):2849–58.
- [21] Topolanek D, Lehtonen M, Adzman MR, Toman P. Earth fault location based on evaluation of voltage sag at secondary side of medium voltage/low voltage transformers. *IET Generat Transm Distribut* 2015;9(14):2069–77.
- [22] Topolanek D, Toman P, Orsagova J. Evaluation method for determining of the probability of an asymmetrical fault location in a distribution network and a monitoring system for performing such method. European patent No. EP2940483 (A1); Priority date: 2014-04-14, European Patent Office.
- [23] Topolanek D, Toman P, Drapela J, Jurak V, Jurik M, Jiricka J. Evaluation of the new method Vdip for an earth fault location. *CIRED 2019 - 25th International Conference and Exhibition on Electricity Distribution*, Madrid, Spain. 2019. p. 1–5.